Irrotational and rotational effects of viscosity on Kelvin-Hemholtz instability for two fluids with small density ratio

J. C. Padrino, D. D. Joseph,* and H. Kim
Department of Aerospace Engineering and Mechanics,
University of Minnesota, Twin Cities Campus, MN, 55455, USA
(Dated: December 22, 2010)

The effects of viscosity on the Kelvin Helmholtz (KH) instability of uniform flow on an unbounded domain are analyzed using two irrotational theories (VPF), an exact rotational theory (ES) and a hybrid rotational/irrotational theory (HS). One of the irrotational theories arises from evaluation of the viscous normal stress on potential flow (VPF1).The second irrotational theory is the dissipation method here derived specially for the KH problem(VPF2). The two irrotational theories give rise to different results. The rotational theory can give rise to KH instability if and only if the gas is inviscid and irrotational (IPF) but the analysis can be extended to account viscous effects by replacing (IPF) with viscous potential flow. To our knowledge quantitave results for KH instability of an unbounded domain are unavailable.

I. INTRODUCTION

Purely irrotational flows are those for which the vorticity is identically zero. The velocity is thus given by the gradient of a harmonic potential. There are *two theories of potential flow of a viscous fluid*, one labeled here as "viscous potential flow" (VPF1) and the other labeled as the "dissipation method" (VPF2). These irrotational theories are distinct. Viscous potential flow is a theory appropriate to two-fluid flows in general and works best for gas-liquid flows. In this theory, the fluids are viscous and the motion is assumed to be irrotational; in particular, viscosity enters the analysis through the viscous irrotational stress in the jump in normal stress across a fluid-fluid interface. The dissipation method, on the other hand, is a well known theory which was introduced by Stokes [1] in his study of the decay of waves. Every irrotational flow, even those outside boundary layers on rigid solids, gives rise to a viscous dissipation whose consequences need study. The dissipation method is based on the fundamental fact that the viscous stresses of the irrotational flow are self-equilibrated and do not give rise to forces in the equations but they do work and give rise to energy and dissipation.

Results of analysis of purely irrotational flow prior to 2007 can be found in the book "Potential flows of viscous and viscoelastic fluids" [2]. These and more recent results are posted as freely downloadable PDF files at http://www.aem.umn.edu/people/faculty/joseph/ViscousPotentialFlow/. Topics of fluid mechanics which have been studied include cavitation [3–5], capillary breakup and rupture [6–8], Rayleigh-Taylor [9] and Kelvin-Helmholtz [10] instabilities, irrotational Faraday waves on a viscous fluid (Ch. 15 in [2]), phase change problems involving heat and mass transfer [11, 12], the viscous decay of capillary-gravity waves [13], oscillations on drops and bubbles [14], waves and rupture of moving thin films [15], Hele-Shaw flows [16], boundary layer theory for flow over rigid solids and flow induced structure of particles in viscous and viscoelastic fluids (see Chapters 18 and 20 in [2] and references therein), rising of a spherical cap bubble [17] and Taylor bubbles in round tubes [18] and other topics.

Which of the two theories is better? We can answer this question after comparing the results given by each theory with the exact solutions and experiments, but we cannot answer this question *a priori*. To complete our theory of the effects of viscosity in irrotational flows we need to answer this question. This is a new question for fluid mechanics researchers who follow Lamb[19] and the works of G.I. Taylor. These authors do the dissipation method VPF2 in some problems of gas-liquid flows but in most other problems involving gas-liquid surfaces, they set the viscosity to zero and neglect the effects of the irrotational viscous normal stress. We think that their approach is greatly flawed.

To bring home this point strongly, consider Fig. 1. VPF2 is in better agreement with the exact solution for progressive waves (long waves) and VPF1 is better for decaying waves (short waves) which do not oscillate. We don't yet know why this is true. The answer is not to be obtained in the fluid mechanics literature; in fact the question is not even posed.

The dissipation method is an approximation that is well known in the fluid mechanics community. It will come as a great surprise to fluid mechanicians that better results than those obtained by VPF2 are frequently obtained by the simpler method VPF1. We do not know how to predict which is better *a priori*. In gas-liquid flows we may assume that the shear stress in the gas is negligible so that no condition need be enforced on the tangential velocity at the free surface, but the shear stress must be zero. This condition is enforced in VPF2. On the other hand, no constraint on the shear stress is invoked for VPF1. In general, one gets an irrotational shear stress from the irrotational analysis. The discrep-

* Also at Department of Mechanical and Aerospace Engineering, University of California, Irvine, Irvine, CA, 92YYY, USA; joseph@aem.umn.edu

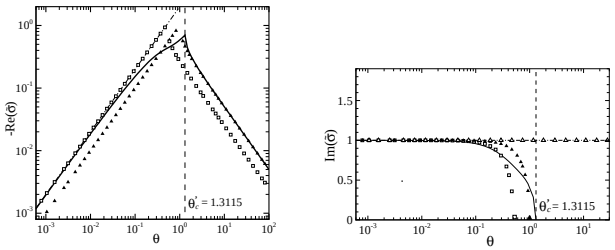

(a) (b)

FIG. 1. Graphs of (a) dimensionless decay rate $-\mathrm{Re}[\tilde{\sigma}]$ and (b) dimensionless frequency $-\mathrm{Im}[\tilde{\sigma}]$ for capillary-gravity waves as a function of the dimensionless parameter $\theta \equiv \nu k^2/\sigma_0$, where ν is the kinematic viscosity of the liquid, σ_0 is the inviscid frequency and $\tilde{\sigma} \equiv \sigma/\sigma_0$: ▲ for VPF1; □ for VPF2; solid line for Lamb's exact solution; dash-dotted line for Lamb's dissipation approximation; △ for inviscid potential flow (IPF) in the figure on the right. Note that Lamb's approximation does not give a cut-off value and the frequency is that for an inviscid liquid. For inviscid flows, the decay rate is zero. The vertical dotted line indicates the critical cut-off value predicted by the exact solution (after [13]).

ancy between this shear stress and the zero shear stress required for exact solutions will generate a vorticity layer. In many cases this layer is small and its influence on the bulk motion and on the irrotational effects of viscosity is minor. In summary, for the irrotational approximation VPF1 the continuity of the normal velocity component and the balance of normal stresses by surface tension are enforced at the interface. For VPF2, in addition to these two interfacial conditions, continuity of the tangential stress is satisfied; because one fluid is inviscid, the tangential stress is zero at the interface. In addition to these three interfacial constraints, the flow of two viscous fluids satisfying the Navier-Stokes equations would also satisfy the continuity of tangential velocity components. This condition is satisfied by neither VPF1 nor VPF2.

Stokes [1] and Lamb [19] used the dissipation method to study the decay of gravity and capillary waves on plane surfaces and spheres. They achieved results for the rate of decay of waves in good agreement with the exact solution in the case of progressive waves. However, their results for the speed of those waves is not correct since the exact solution shows that the speed of progressive waves depends on the viscosity and there is a cut-off wavenumber above which the speed of the waves goes to zero and the progressive waves are replaced by standing waves. When the potential flow solution is carried out correctly (see [13]) results just like the exact solution, uniform in the wavenumber are obtained. The progressive waves, which are associated with long waves, are given by VPF2 and the standing waves, which are associated with short waves, where the cut-off wavenumber is a decreasing function of the viscosity, are given by VPF1. The exact solution is well approximated by potential flow, but different potential flow theories are required (Fig. 1).

Another example is the work on capillary instability in [7, 8] comparing the performance of VPF1, which was formulated in [6], and VPF2; they concluded that VPF2 predicts the growth rate for the most unstable wave in better agreement with the exact solution of the linearized Navier–Stokes equations than VPF1. The approximation deteriorates if the viscosities of the fluids on each side of the interface become of the same order of magnitude. It is also worth mentioning the computation of the drag on a rising bubble. Moore [20] assumed potential flow around the bubble and computed the drag by integrating the irrotational normal stress including the viscous component and obtained $8\pi U\mu a$, where a is the bubble radius, U its rising speed and μ the liquid viscosity. Levich [21] used the dissipation method and obtained a drag of $12\pi U\mu a$. It is not possible *a priori* to predict whether the factor 8 or 12 is better, but comparison with experiments and the boundary layer analysis of Moore [22] favor 12.

A. Self-equilibration of the irrotational viscous stress

The stress in a Newtonian incompressible fluid is given by

$$\mathbf{T} = -p\mathbf{1} + \mu\left(\nabla\mathbf{u} + (\nabla\mathbf{u})^T\right). \tag{1}$$

Most flows have an irrotational viscous stress. The irrotational viscous stress $\boldsymbol{\tau}_I = 2\mu\nabla\otimes\nabla\phi$ does not give rise to a force density term; it does not enter into the equations of motion. The divergence of $\boldsymbol{\tau}_I$ vanishes on each and every point in the domain V of flow. Even though an irrotational viscous stress exists, it does not produce a net force to drive motions. Moreover,

$$\int_V \nabla\cdot\boldsymbol{\tau}_I dV = \int_A \mathbf{n}\cdot\boldsymbol{\tau}_I dS = 0. \tag{2}$$

The traction vector $\mathbf{n}\cdot\boldsymbol{\tau}_I$ have no net resultant on each and every closed surface A in the domain V of flow. We say that the irrotational viscous stresses, which do not drive motions, are self-equilibrated. Irrotational viscous stresses are not equilibrated at boundaries and they may produce forces there. An implication of (2) is that *no force can be produced on a body in steady flow by the viscous irrotational stresses.* This can be called a generalized D'Alembert Paradox. Irrotational viscous torques on bodies also vanish because

$$\int_A \epsilon_{ijk}x_j\tau_{kl}n_l dS = \int_V \frac{\partial(\epsilon_{ijk}x_j\tau_{kl})}{\partial x_l}dV = 0. \tag{3}$$

The key to understanding purely irrotational flows is that even though the irrotational stresses are self-equilibrated the power of these irrotational stress is pos-

itive,

$$\int_A \mathbf{n}\cdot\boldsymbol{\tau}_I\cdot\nabla\phi dV = \int_A n_i\tau_{ij}\frac{\partial\phi}{\partial x_j}dS = \int_V 2\mu\frac{\partial^2\phi}{\partial x_i\partial x_j}\frac{\partial^2\phi}{\partial x_i\partial x_j}dV. \quad (4)$$

From what has just been said, it follows that the Navier–Stokes equations are not the appropriate starting place for the analysis of purely irrotational effects on the dissipation of energy. The correct starting place for this analysis is the energy equation for the Navier–Stokes equation rather than these equations themselves.

B. The rate of change of kinetic energy is not Galilean invariant but the mechanical energy equation is invariant

Consider a free stream of a fluid 1 moving to the right with velocity U_1 underneath another free stream of a fluid 2 moving to the right with velocity U_2 with respect to the laboratory frame $\{x,t\}$. Consider the Galilean transformation,

$$\tilde{\mathbf{x}} = \mathbf{x} - \mathbf{V}t, \quad (5)$$

$$\tilde{t} = t. \quad (6)$$

Hence,

$$\tilde{\mathbf{u}} = \mathbf{u} - \mathbf{V}. \quad (7)$$

where $\{\tilde{x},\tilde{t}\}$ denotes a reference frame moving with constant velocity V with respect to the laboratory frame. In particular, for $\mathbf{V} = (V,0,0)$ an observer traveling with the moving frame will see two streams with velocities $\tilde{U}_1 = U_1 - V$ and $\tilde{U}_2 = U_2 - V$, respectively. After applying the Galilean transformation above to the Navier–Stokes equations we have that these equations are invariant. This is a manifestation of the fundamental view that any physical law should take the same form in any inertial frame of reference. Also, the boundary conditions for the motion at an interface (continuity of tangential and normal velocity components, continuity of tangential stresses and balance of normal stresses by surface tension) are all invariant.

On the other hand, for the rate of change of the kinetic energy we have

$$\frac{d}{dt}\frac{|\mathbf{u}|^2}{2} = \mathbf{u}\cdot\frac{d\mathbf{u}}{dt} = (\tilde{\mathbf{u}}+\mathbf{V})\cdot\frac{d\tilde{\mathbf{u}}}{d\tilde{t}} = \frac{d}{d\tilde{t}}\frac{|\tilde{\mathbf{u}}|^2}{2} + \mathbf{V}\cdot\frac{d\tilde{\mathbf{u}}}{d\tilde{t}} \quad (8)$$

Therefore, because of the last term in (8), the rate of change of the kinetic energy is not invariant. However, the energy equation for

$$\rho\mathbf{u}\cdot\frac{d\mathbf{u}}{dt} = \mathbf{u}\cdot(\nabla\cdot\mathbf{T}) \quad (9)$$

is transformed to

$$\rho\tilde{\mathbf{u}}\cdot\frac{d\tilde{\mathbf{u}}}{d\tilde{t}} + \mathbf{V}\cdot\frac{d\tilde{\mathbf{u}}}{d\tilde{t}} = \tilde{\mathbf{u}}\cdot\left(\tilde{\nabla}\cdot\tilde{\mathbf{T}}\right) + \mathbf{V}\cdot\left(\tilde{\nabla}\cdot\tilde{\mathbf{T}}\right) \quad (10)$$

where

$$\mathbf{T} = -p\mathbf{1} + 2\mu\mathbf{D} = -\tilde{p}\mathbf{1} + 2\mu\tilde{\mathbf{D}} = \tilde{\mathbf{T}}. \quad (11)$$

The symbol "˜" denotes quantities with respect to the moving frame. Here, $\mathbf{D}$ and $\tilde{\mathbf{D}}$ denote the symmetric part of the velocity gradients $\nabla\mathbf{u}$ and $\tilde{\nabla}\tilde{\mathbf{u}}$, respectively. Also, $\tilde{p} = p$. Because the Navier–Stokes equations are invariant, we obtain, from (10),

$$\rho\tilde{\mathbf{u}}\cdot\frac{d\tilde{\mathbf{u}}}{d\tilde{t}} = \tilde{\mathbf{u}}\cdot\left(\tilde{\nabla}\cdot\tilde{\mathbf{T}}\right). \quad (12)$$

Therefore, for a flow that is governed by the incompressible Navier–Stokes equations, its associated energy equation is also Galilean invariant. Because the velocity is divergence free, expression (12) may be rewritten as

$$\rho\tilde{\mathbf{u}}\cdot\frac{d\tilde{\mathbf{u}}}{d\tilde{t}} = \rho\frac{d}{d\tilde{t}}\frac{|\tilde{\mathbf{u}}|}{2}^2 = \tilde{\nabla}\cdot\left(\tilde{\mathbf{T}}\cdot\tilde{\mathbf{u}}\right) - 2\mu\tilde{\mathbf{D}}:\tilde{\mathbf{D}}, \quad (13)$$

where the last term gives the viscous dissipation of energy.

C. Four theories of the Kelvin-Helmholtz instability

Two parallel infinite fluid streams of different velocities give rise to the Kelvin-Helmholtz instability. In the analysis of this instability, the fluids are usually assumed to be inviscid because the velocity discontinuity would be smoothed by viscosity. Viscous effects have been included by many authors through empirical correlations for the interfacial stress. Nevertheless, comparison with experiments has not been convincing (see the review in [23]).

To the best of our knowledge, the only work in which the effects of the viscosity of the fluids on both sides of the interface on the Kelvin-Helmholtz instability have been considered is the model by Funada and Joseph [10]. They considered purely irrotational flow above and below the velocity discontinuity. The only place where viscosity enters is in the evaluation of the viscous normal stress at the interface. This analysis has been named "viscous potential flow" (VPF1). It should be mentioned here that viscous effects on the stability of the flow of two plane-parallel streams have been investigated using numerical analysis considering a continuous, smooth variation of the basic velocity from one value to the other. For instance, [24] considered a velocity variation according to a hyperbolic tangent law of the spatial coordinate normal to the interface. However, in these cases the sharp discontinuity of the velocity profile is smoothed out. That is, the velocity profile subject of analysis does not correspond to that of the Kelvin-Helmholtz instability. On the other hand, in the work by [10], viscosity on both sides of the interface enters the analysis while the basic profile remains discontinuous.

Another approach to the analysis of the Kelvin-Helmhotlz instability is to consider one fluid as viscous and the other as inviscid. The advantage of this method is that it leads to an exact solution (ES) of the Navier–Stokes equations; hence, vorticity is not zero on the viscous side. This type of analysis has been conducted by [25] for the case of a viscous film in an inviscid ambient fluid, and by [26] to model the dynamics of a moving inviscid fluid sharing an interface with a viscous liquid, including the effects of heat and mass transfer.

The method described in the previous paragraph can be generalized by treating both fluids as viscous, constraining the flow of one of the fluids to be irrotational whereas the flow of the other fluid will have vorticity[27]. This simply translates into a modification of the interfacial dynamic conditions: The viscous irrotational stress will enter the jump of the normal component of the stress across the interface, and the tangential component will not vanish at the interface. This analysis is termed here as the "hybrid method" (HM).

In this work we introduce yet another approach, the dissipation method (VPF2), to the analysis of the Kelvin-Helmholtz instability. Unlike previous formulations by other authors (see below), the analysis of irrotational dissipation leads to a determination of the effects of viscosity on the wavespeed. The analysis starts from an energy balance in integral form written for each fluid stream obtained from the "dot" product of the velocity perturbation with the linearized incompressible Navier–Stokes equations. As in the exact solution, one fluid is set to be inviscid and the other viscous, with gravity pointing from the inviscid to the viscous. The interfacial constraints for the normal velocity and stress and the tangential stress satisfied by the exact solution are enforced in the energy balance. Next, the integrals are evaluated in potential flow. The analysis yields a dispersion relation for the growth rate and wave frequency that includes viscous effects. This dispersion relation is different from that obtained by VPF1. Because for ES and VPF2 the fluid at the top is assumed to be inviscid, the different methods considered here are applied to a pair of fluids with a very small upper-fluid to lower-fluid density ratio. That is, for gas-liquid flows. Results from ES, HM and VPF2 are computed for a given velocity profile, neglecting stabilizing effects of interfacial tension and gravity. Results from VPF1 by [10] and the classical theory for inviscid fluids are also given here.

II. ANALYSIS

A. Problem formulation and governing equations

Consider two parallel streams of two different incompressible fluids. Fluid 1 has density ρ_1 and viscosity μ_1 and moves with constant velocity $\mathbf{U}_1 = U_1\mathbf{i}$. Fluid 2 has density ρ_2 and is considered to be inviscid, i.e. $\mu_2 = 0$, and moves with velocity $\mathbf{U}_2 = U_2\mathbf{i}$ also constant. Orthogonal unit vectors $\{\mathbf{i}, \mathbf{j}\}$ point along the positive x and y directions, respectively (Fig. 2). The position of the plane infinite interface separating fluid 1 from fluid 2 is $y = 0$; fluid 1 occupies the $y < 0$ semi-infinite space and fluid 2 occupies the $y > 0$ semi-infinite space. The interface is characterized by a constant interfacial tension γ. Gravity g acts in the y-direction and points from fluid 2 to fluid 1. We consider a two-dimensional motion. Suppose now that the interface is slightly perturbed so that its new position is $y = \eta(x, t)$ and let $\mathbf{u} = u\mathbf{i} + v\mathbf{j}$ and p be the velocity and pressure perturbations, respectively. The governing equations are the incompressible Navier–Stokes equations written for each fluid with appropriate boundary conditions. In the far field, the perturbations vanish. At the interface, the balance of normal stresses by interfacial tension effects, continuity of tangential stresses and normal velocity components are enforced. No condition is imposed on the tangential velocity components, to allow for the discontinuity in the base velocity across the interface. This follows the approach in Ref. [26].

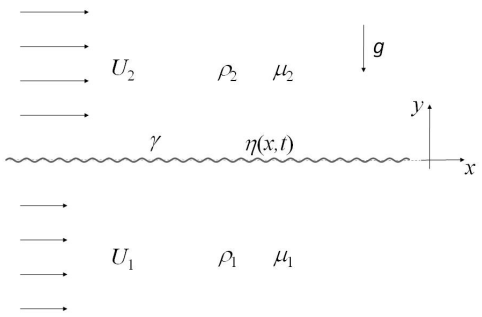

FIG. 2. Sketch of the geometry of the problem showing two parallel streams of fluids 1 and 2 having velocities U_1 and U_2, respectively, and the Cartesian reference frame. Each fluid has density and viscosity ρ_j and μ_j, $j = 1, 2$, and γ is the (constant) interfacial tension. The position of the perturbed interface is denoted by $y = \eta(x, t)$. In some cases, the viscosity $\mu_2 = 0$.

Linearization of the governing equations and boundary conditions, after subtracting the base state, leads to

$$\rho\left(\frac{\partial \mathbf{u}}{\partial t} + \mathbf{U}\cdot\nabla\mathbf{u}\right) = -\nabla p + \mu\nabla^2\mathbf{u}, \tag{14}$$

$$\nabla\cdot\mathbf{u} = 0, \tag{15}$$

for each fluid, with $\mu_2 = 0$, together with boundary conditions

$$\left(-p_1 + 2\mu_1\frac{\partial v_1}{\partial y}\right) + p_2 = \gamma\frac{\partial^2\eta}{\partial x^2} - (\rho_1 - \rho_2)g\eta, \tag{16}$$

$$\frac{\partial u_1}{\partial y} + \frac{\partial v_1}{\partial x} = 0, \tag{17}$$

$$v_1 = \frac{\partial\eta}{\partial t} + U_1\frac{\partial\eta}{\partial x} \qquad \text{and} \qquad v_2 = \frac{\partial\eta}{\partial t} + U_2\frac{\partial\eta}{\partial x}, \tag{18}$$

at $y = 0$ from the balance of the jump in normal stresses by interfacial tension, continuity of tangential stresses, and continuity of normal velocity components along with the kinematic condition, respectively.

B. Exact solution – Inviscid fluid above

Using normal mode expressions for the variables, the analysis of the linearized governing equations (14)–(18) described in the A leads to the following dispersion relation

$$Y^4 + a_2 Y^2 + a_1 Y + a_0 = 0, \tag{19}$$

where

$$\begin{aligned} a_0 =& 2\mathrm{i}\alpha_2 \frac{(U_1 - U_2)}{k\nu_1} - \alpha_2 \frac{(U_1 - U_2)^2}{k^2\nu_1^2}, \\ &+ (\alpha_1 - \alpha_2)\, Q + Q^{1/3} S + 1, \\ a_1 =& -2(\alpha_1 - \alpha_2) - 2, \\ a_2 =& 2(\alpha_1 - \alpha_2) - 2\mathrm{i}\alpha_2 \frac{(U_1 - U_2)}{k\nu_1}, \end{aligned}$$

and

$$\begin{aligned} Y &= \sqrt{1 + \frac{\sigma + \imath k U_1}{k^2\nu_1}} = \frac{q_1}{k}, \quad \text{so that} \\ \sigma &= k^2\nu_1 \left(Y^2 - 1\right) - \imath k U_1, \\ \alpha_1 &= \frac{\rho_1}{\rho_1 + \rho_2}, \quad \alpha_2 = \frac{\rho_2}{\rho_1 + \rho_2}, \\ Q &= \frac{g}{k^3\nu_1^2}, \quad \text{and} \quad Q^{-2/3} S = \frac{k^2\gamma}{g(\rho_1 + \rho_2)}. \end{aligned}$$

In writing (19), the term $(Y^2 - 1)$ has been factored out because it gives the root $Y = -1$, which is inadmissible, and the root $Y = 1$, which is trivial.

If in the analysis by Ref. [26] heat and mass transfer are discarded from the model, their (quintic) dispersion relation (23) reduces to our quartic equation (19) after the term $(Y + 1)$ is factored out from their formula.

Also, expression (19), with $U_1 = U_2 = 0$, reduces to that of [28] (Sec. 94, pp. 443), when we set $\mu_2 = 0$ in his formula for the Rayleigh-Taylor instability for two viscous fluids. In addition, if we set $\rho_2 = 0$ in (19), we obtain the quartic dispersion relation given by [19], in his study of capillary-gravity waves.

C. Hybrid method – Irrotational flow of a viscous fluid above

A generalization of the analysis presented in the previous section can be developed by considering that fluid 2 is viscous and its motion is irrotational. The interfacial conditions must be modified accordingly. In the balance of normal stresses (16) the viscous irrotational normal stress on the fluid-2 side must be added to the hydrodynamic pressure. That is,

$$\begin{aligned} \left(-p_1 + 2\mu_1 \frac{\partial v_1}{\partial y}\right) - \left(-p_2 + 2\mu_2 \frac{\partial v_2}{\partial y}\right) \\ = \gamma \frac{\partial^2 \eta}{\partial x^2} - (\rho_1 - \rho_2) g\eta. \end{aligned} \tag{20}$$

With respect to the continuity of tangential stresses across the interface, the tangential component of the (rotational) stress on the fluid-1 side does not vanish; instead, it equals the tangential component of the (irrotational) stress on the fluid-2 side, i.e.

$$\mu_1 \left(\frac{\partial u_1}{\partial y} + \frac{\partial v_1}{\partial x}\right) = \mu_2 \left(\frac{\partial u_2}{\partial y} + \frac{\partial v_2}{\partial x}\right). \tag{21}$$

With these two modifications, following the preceding analysis leads to the dispersion relation

$$Y^5 + Y^4 + a_3 Y^3 + a_2 Y^2 + a_1 Y + a_0 = 0, \tag{22}$$

where

$$\begin{aligned} a_0 =& 1 + 2\mathrm{i}\alpha_2 \frac{(U_1 - U_2)}{\nu_1 k} - \alpha_2 \frac{(U_1 - U_2)^2}{\nu_1^2 k^2} \\ &- 4m\alpha_2 - 4\mathrm{i}m\alpha_2 \frac{(U_1 - U_2)}{\nu_1 k} + (\alpha_1 - \alpha_2) Q + Q^{1/3} S, \\ a_1 =& -1 - 2(\alpha_1 - \alpha_2) + 2\mathrm{i}\alpha_2 \frac{(U_1 - U_2)}{\nu_1 k} \\ &- \alpha_2 \frac{(U_1 - U_2)^2}{\nu_1^2 k^2} + (\alpha_1 - \alpha_2) Q + Q^{1/3} S, \\ a_2 =& -2 - 2\mathrm{i}\alpha_2 \frac{(U_1 - U_2)}{\nu_1 k} + 4m\alpha_2, \\ a_3 =& 2(\alpha_1 - \alpha_2) - 2\mathrm{i}\alpha_2 \frac{(U_1 - U_2)}{\nu_1 k}, \end{aligned}$$

and $m = \nu_2/\nu_1$ is the kinematic viscosity ratio. After setting $m = 0$, the root $Y = -1$ (inadmissible) can be factored out of (22), and this quintic equation reduces to the quartic equation (19).

D. Dissipation method

The following method for constructing the analysis of the dissipation of energy was introduced by [13]; unlike other dissipation approaches found in the fluid mechanics literature, it gives rise to complex eigenvalues, growth rates and wavespeeds. This method starts with an energy identity for solutions of the Navier-Stokes equation without assuming anything about irrotationality or vorticity. Only after a general energy integral relation including the dissipation integral is obtained, the viscous potential flow will be used to substitute for the velocity derivatives in the various integrals.

Taking the "dot" product of the linearized momentum equation (14) with the complex conjugate of the velocity perturbation, and integrating this equation for fluid

1 over volume $V_1 \equiv \{-\infty < y < 0, x_0 < x < x_0 + \lambda\}$ and that for fluid 2 over volume $V_2 \equiv \{0 < y < \infty, x_0 < x < x_0 + \lambda\}$, with (x_0, y_0) arbitrary, yields a mechanical energy balance statement for each fluid. Adding the energy balances for fluids 1 and 2 leads to

$$\int_{V_1} \rho_1 \bar{\mathbf{u}}_1 \cdot \left(\frac{\partial \mathbf{u}_1}{\partial t} + \mathbf{U}_1 \cdot \nabla \mathbf{u}_1 \right) dV + \int_{V_2} \rho_2 \bar{\mathbf{u}}_2 \cdot \left(\frac{\partial \mathbf{u}_2}{\partial t} + \mathbf{U}_2 \cdot \nabla \mathbf{u}_2 \right) dV = \int_A \mathbf{j} \cdot \mathbf{T}_1 \cdot \bar{\mathbf{u}}_1 dA - \int_A \mathbf{j} \cdot \mathbf{T}_2 \cdot \bar{\mathbf{u}}_2 dA - \int_{V_1} 2\mu_1 \mathbf{D}_1 : \bar{\mathbf{D}}_1 dV. \quad (23)$$

Here, $\mathbf{e}_j = \mathbf{e}_1 = \mathbf{j}$ for fluid 1 and $\mathbf{e}_j = \mathbf{e}_2 = -\mathbf{j}$ for fluid 2; the stress $\mathbf{T} = -p\mathbf{1} + 2\mu\mathbf{D}$, and $\mathbf{D}$ is the symmetric part of $\nabla\mathbf{u}$. Viscosity $\mu_2 = 0$ for fluid 2. Symbol "$\bar{\ }$" denotes complex conjugate. The surface integrals over the region A of the *unperturbed* interface are obtained by applying the divergence theorem, periodicity of the flow in the x direction and the vanishing of the velocity perturbation in the far field. The last term in (23) denotes the energy viscous dissipation, which only appears for fluid 1. This form of obtaining an energy balance by using the complex conjugate of the velocity follows that by [29] (see §6.7.4, p. 177) in the analysis of the Rayleigh-Taylor instability.

Consider the surface integrals on the right-hand side of (23). Writing $\bar{\mathbf{u}}$ in terms of its Cartesian components $\bar{\mathbf{u}} = \bar{u}\mathbf{i} + \bar{v}\mathbf{j}$ and using boundary condition (17) for the vanishing of the tangential stress (i.e. $\mathbf{j} \cdot \mathbf{T}_1 \cdot \mathbf{i} = 0$) and the fact that $\mathbf{j} \cdot \mathbf{T}_2 \cdot \mathbf{i} = 0$ for an inviscid fluid, we can write

$$\int_A \mathbf{j} \cdot \mathbf{T}_1 \cdot \bar{\mathbf{u}}_1 dA - \int_A \mathbf{j} \cdot \mathbf{T}_2 \cdot \bar{\mathbf{u}}_2 dA = \int_A \left[\mathbf{j} \cdot \mathbf{T}_1 \cdot \mathbf{j}\ \bar{v}_1 - \mathbf{j} \cdot \mathbf{T}_2 \cdot \mathbf{j}\ \bar{v}_2 \right] dA. \quad (24)$$

With the balance of normal stresses in (16) written as

$$\mathbf{j} \cdot \mathbf{T}_1 \cdot \mathbf{j} - \mathbf{j} \cdot \mathbf{T}_2 \cdot \mathbf{j} = \gamma \frac{\partial^2 \eta}{\partial x^2} - (\rho_1 - \rho_2) g\eta, \quad (25)$$

eliminating $\bar{v}_1$ and $\bar{v}_2$ with condition (18), and using (25) to eliminate the normal stress on the viscous side $\mathbf{j} \cdot \mathbf{T}_1 \cdot \mathbf{j}$ in favor of that on the inviscid side $\mathbf{j} \cdot \mathbf{T}_2 \cdot \mathbf{j}$, expression (24) becomes

$$\int_A \left[\mathbf{j} \cdot \mathbf{T}_1 \cdot \mathbf{j}\ \bar{v}_1 - \mathbf{j} \cdot \mathbf{T}_2 \cdot \mathbf{j}\ \bar{v}_2 \right] dA = \int_A \left[\gamma \frac{\partial^2 \eta}{\partial x^2} - (\rho_1 - \rho_2) g\eta \right] \left[\frac{\partial \bar{\eta}}{\partial t} + U_1 \frac{\partial \bar{\eta}}{\partial x} \right] dA + \int_A \mathbf{j} \cdot \mathbf{T}_2 \cdot \mathbf{j} \, (U_1 - U_2) \frac{\partial \bar{\eta}}{\partial x} dA. \quad (26)$$

With (26), the boundary conditions satisfied by ES have also been enforced in the integral balance (26).

From the "exact solution" analysis (ES), we have that the flow field $\mathbf{u}_2$ for the inviscid fluid 2 is irrotational whereas, for fluid 1, $\mathbf{u}_1$ is not. Therefore, we can set $\mathbf{u}_2 = \nabla\phi_2$, where ϕ_2 is harmonic. In expression (26), there is an integral involving $\mathbf{j} \cdot \mathbf{T}_2 \cdot \mathbf{j} = -p_2$. From the linearized momentum equation in (14) for fluid 2, we can integrate and find that

$$-p_2 = \rho_2 \left(\frac{\partial \phi_2}{\partial t} + U_2 \frac{\partial \phi_2}{\partial x} \right) \quad (27)$$

up to a function of time. Use of (27) results in no loss of generality.

So far, we have set no constraint on the vorticity of the flow. From ES, the flow field for fluid 1 is rotational. In what follows, the integrals are evaluated in an approximate manner by neglecting vorticity. Thus, the velocity field for fluid 1 is approximated as the gradient of a potential, $\mathbf{u}_1 = \nabla\phi_1$. Letting

$$\begin{aligned} \phi_1(x, y, t) &= A_1 \exp(ky) \exp(\sigma t + \mathrm{i}kx), \\ \phi_2(x, y, t) &= A_2 \exp(-ky) \exp(\sigma t + \mathrm{i}kx), \end{aligned} \quad (28)$$

using conditions (18), and expression

$$\eta(x, t) = \eta_0 \exp(\sigma t + \mathrm{i}kx), \quad (29)$$

for η we find

$$\begin{aligned} kA_1 &= \ \ (\sigma + \mathrm{i}kU_1)\eta_0, \\ kA_2 &= -(\sigma + \mathrm{i}kU_2)\eta_0. \end{aligned} \quad (30)$$

For potential flow, after applying the divergence theorem, periodicity of the potential in x and the vanishing of the velocity perturbation in the far field, the left-hand side of (23) becomes,

$$\int_{V_1} \rho_1 \bar{\mathbf{u}}_1 \cdot \left(\frac{\partial \mathbf{u}_1}{\partial t} + \mathbf{U}_1 \cdot \nabla \mathbf{u}_1 \right) dV + \int_{V_2} \rho_2 \bar{\mathbf{u}}_2 \cdot \left(\frac{\partial \mathbf{u}_2}{\partial t} + \mathbf{U}_2 \cdot \nabla \mathbf{u}_2 \right) dV = \int_A \rho_1 \bar{v}_1 \left(\frac{\partial \phi_1}{\partial t} + U_1 \frac{\partial \phi_1}{\partial x} \right) dA - \int_A \rho_2 \bar{v}_2 \left(\frac{\partial \phi_2}{\partial t} + U_2 \frac{\partial \phi_2}{\partial x} \right) dA, \quad (31)$$

where $v_j = \mathbf{j} \cdot \nabla\phi_j = \partial\phi_j/\partial y$, with $j = 1, 2$. For the dissipation integral, in potential flow, the following relation holds,

$$\int_{V_1} 2\mu_1 \mathbf{D}_1 : \bar{\mathbf{D}}_1 dV = \int_A 2\mu_1 \mathbf{j} \cdot \mathbf{D}_1 \cdot \bar{\mathbf{u}}_1 dA, \quad (32)$$

and the right-hand side of expression (26) is also evaluated in potential flow.

Evaluating the integrals in (26), (31) and (32), with the aid of (28)-(30), and substituting back in (23), yields, after some rearranging,

$$\left[\rho_1 (\sigma + \mathrm{i}kU_1)^2 + \rho_2 (\sigma + \mathrm{i}kU_2)^2 + \gamma k^3 + (\rho_1 - \rho_2) gk + 4\mu_1 k^2 (\sigma + \mathrm{i}kU_1) \right] [\bar{\sigma} - \mathrm{i}kU_1] = 0. \quad (33)$$

Therefore, the dispersion relation from VPF2 may be written as

$$\rho_1 \left(\sigma + \mathrm{i}kU_1\right)^2 + \rho_2 \left(\sigma + \mathrm{i}kU_2\right)^2 + \gamma k^3 + (\rho_1 - \rho_2)gk + 4\mu_1 k^2 \left(\sigma + \mathrm{i}kU_1\right) = 0, \quad (34)$$

which is quadratic, after discarding the neutrally stable root $\sigma + \mathrm{i}kU_1 = 0$. When the liquid viscosity μ_1 is set to zero, this dispersion relation reduces to the eigenvalue relation for the classical Kelvin-Helmholtz instability (e.g., see [30], pp. 28). On the other hand, if we set $U_1 = U_2 = 0$ and set $\rho_2 = 0$ for a viscous liquid in (34), this reduces to the dispersion relation governing the dynamics of capillary-gravity waves from VPF2 (see [13]).

E. Viscous potential flow

The VPF1 analysis of the Kelvin-Helmholtz instability was conducted by [10] (see also Ch. 11 in [2]). There, irrotational viscous normal stresses are included in the (pointwise) balance of normal stresses at the interface for two viscous fluids assuming potential flow. Balance laws in integral form—which are used in the case of VPF2—are not considered in VPF1. The dispersion relation from VPF1 is

$$\rho_1 \left(\sigma + ikU_1\right)^2 + \rho_2 \left(\sigma + ikU_2\right)^2 + 2\mu_1 k^2 \left(\sigma + ikU_1\right) + 2\mu_2 k^2 \left(\sigma + ikU_2\right) + \gamma k^3 + (\rho_1 - \rho_2)gk = 0. \quad (35)$$

Relation (34) from VPF2 has the same form as the dispersion relation from VPF1, except that a factor of two was obtained from VPF1 for the viscous terms rather than the factor of four obtained here from VPF2.

III. RESULTS AND DISCUSSION

In this section we present results for the growth rate and wave frequency from the dispersion relations presented in the previous section for VPF1, VPF2, ES and HM. Here, we also include predictions from the classical theory where both fluids are inviscid, designated as "inviscid potential flow" (IPF). Instead of applying the dispersion relations to the original basic velocity profile, we apply them to the profile seen by an observer moving with the average velocity $(U_1 + U_2)/2$. With respect to this moving frame, fluid 1 moves with velocity $U = (U_1 - U_2)/2$ and fluid 2 with velocity $-U$. Under a Galilean transformation, the growth rate is invariant and, in this case, the wavespeed in the original frame differs from that in the moving frame by the average velocity. With no loss of generality, the original basic velocity profile can be set in such a way that $U > 0$.

The results are presented in dimensionless form. The dimensionless complex growth rate is defined as

$$\hat{\sigma} = \frac{\sigma}{kU}, \quad (36)$$

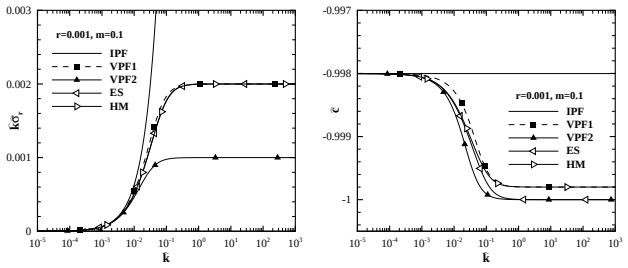

(a) (b)

FIG. 3. Graphs of (a) dimensionless growth rate $\hat{k}\hat{\sigma}_r$ and (b) dimensionless wavespeed $\hat{c}$ vs. dimensionless wavenumber $\hat{k}$ from five methods, namely, IPF, VPF1, VPF2, ES, and HM, for a pair of fluids with density ratio $r = 0.001$ and kinematic viscosity ratio $m = 0.1$. Surface tension and gravity are neglected. Only the roots with positive growth rate are shown here.

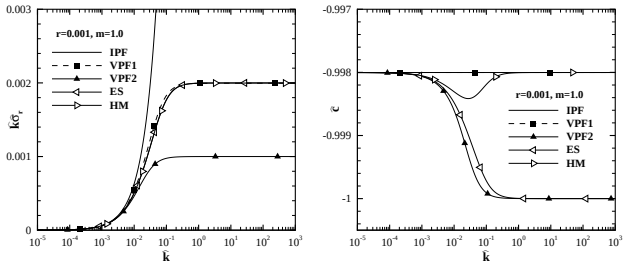

(a) (b)

FIG. 4. Graphs of (a) dimensionless growth rate $\hat{k}\hat{\sigma}_r$ and (b) dimensionless wavespeed $\hat{c}$ vs. dimensionless wavenumber $\hat{k}$ from five methods, namely, IPF, VPF1, VPF2, ES, and HM, for a pair of fluids with density ratio $r = 0.001$ and kinematic viscosity ratio $m = 1.0$. Surface tension and gravity are neglected. Only the roots with positive growth rate are shown here.

so that the dimensionless growth rate is $\hat{\sigma}_r = \mathrm{Re}[\hat{\sigma}]$ and the dimensionless wavespeed is $\hat{c} = \mathrm{Im}[\hat{\sigma}]$. Figs. 3–5 show the variation of the product $\hat{k}\hat{\sigma}_r$ and $\hat{c}$ with a dimensionless wavenumber defined as

$$\hat{k} = \frac{\nu_1 k}{U}, \quad (37)$$

for a fixed density ratio $r = 0.001$, which can be identified with a liquid-gas system (e.g., water-air) and three different values of the kinematic viscosity ratio, namely, $m = 0.1$ (e.g., viscous oil-air), $m = 1$, and $m = 10$ (e.g., water-air). Even though for a typical gas-liquid system the dynamic viscosity ratio is in the order of 10^{-2} or smaller, depending upon how viscous the liquid can be, kinematic viscosity ratios in the order of 1 or 10 can be realized. The product $\hat{k}\hat{\sigma}_r$ also designates a dimensionless growth rate.

From the dispersion relations written in dimensionless form in the B, the dimensionless growth rate and

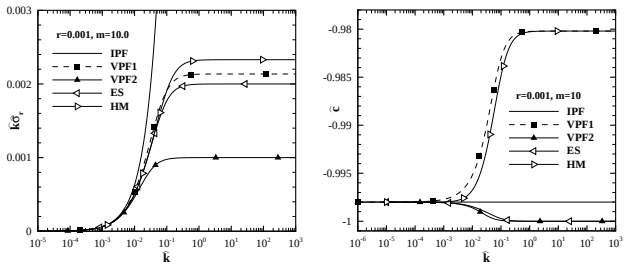

(a) (b)

FIG. 5. Graphs of (a) dimensionless growth rate $\hat{k}\hat{\sigma}_r$ and (b) dimensionless wavespeed $\hat{c}$ vs. dimensionless wavenumber $\hat{k}$ from five methods, namely, IPF, VPF1, VPF2, ES, and HM, for a pair of fluids with density ratio $r = 0.001$ and kinematic viscosity ratio $m = 10.0$. Surface tension and gravity are neglected. Only the roots with positive growth rate are shown here.

wavespeed depends only on the density ratio r in the case of IPF. For VPF2 and ES, they depend on r and the dimensionless wavenumber $\hat{k}$. For VPF1 and HM, they depend on $\hat{k}$, r and the kinematic viscosity ratio m.

These figures show that $\hat{k}\hat{\sigma}_r$ growths unbounded as $\hat{k}$ increases for IPF. According to the classical theory for inviscid fluids, as explained in the B using definition (B2), the discontinuous basic flow is Hadamard unstable because the growth rate increases linearly with the wavenumber. Therefore, the waves become more unstable as they become shorter. On the other hand, results from the theories that account for viscous effects show that viscosity does not stabilize short waves but the instability is not of the Hadamard type. The numerical results in Figs. 3–5 and the analytical expressions for large $\hat{k}$ in the B, demonstrate that the growth rate tends to an asymptotic value that varies with each theory.

For a kinematic viscosity ratio $m = 0.1$ and $m = 1$, VPF1, ES and HM predict similar results as the wavenumber increases. The growth rate from VPF2, on the other hand, is about half of those results [Figs. 3(a) and 4(a)]. This is in agreement with the analytical results for the asymptotes, given in the B. For $m = 10$, the graphs of the growth rate in Fig. 5(a) show that the differences in the predictions from the various theories become noticeable as the dimensionless wavenumber increases, a result confirmed by the expressions for large $\hat{k}$ in that Appendix. There, it is shown that discrepancies between VPF1, ES and HM will be significant only when m is large, for fixed r.

For the wavespeed, for m =0.1, all viscous theories produce similar results [Fig. 3(b)]. The wavespeed slightly increases as the wavelength becomes shorter. In general, for the wavespeed, VPF1 exhibits the same trend of HM as $\hat{k}$ changes, whereas VPF2 follows that by ES, as predicted by the analytic expressions for large $\hat{k}$. For IPF, the wavespeed is independent of the wavenumber. When both fluids have the same kinematic viscosity ($m = 1$), VPF1 predicts the same wavespeed as the inviscid theory for all wavelengths. Moreover, for short waves, HM also matches the results from the inviscid theory, as shown in Fig. 4(b) (see also analytical results in B). For $m = 10$, i.e. when the kinematic viscosity of fluid 2 is larger than that of fluid 1, VPF1 and HM, which are the two theories that account for the viscosity of both fluids, predicts that shorter waves are slower than long waves, contrary to the trend resulting from VPF2 and ES, the two theories that consider fluid 2 as inviscid [Fig. 5(b)].

In sum, when the kinematic viscosity on one side is much smaller than that on the other side, viscous effects on that side are weak, so that results from HM and ES agree well. In this particular scenario, these rotational theories seem to be the best possible model of the Kelvin-Helmholtz instability. With respect to the viscous irrotational theories, VPF1 shows very good agreement with the rotational solutions for the interval of wavenumbers considered, whereas VPF2 is off the mark in terms of predicting the growth rate. Discrepancies become significant as the kinematic viscosity ratio increases.

ACKNOWLEDGMENTS

The authors have greatly profited from conversations and correspondence on related topics with Prof. W. A. Sirignano. The authors acknowledge support from the Applied Mathematics Division of the National Science Foundation under ARRA. This research has been partially supported by the US Army Research Office through grant No. W911NF-06-1-0225 and W911NF-09-1-0208, with Dr. Kevin McNesby and Dr. Ralph Anthenien having served sequentially as program managers.

Appendix A: Exact solution

Here, details of the derivation of the dispersion relation in (19) are presented. Using normal modes, we may write, for the interface position

$$\eta(x,t) = \eta_0 \exp(\sigma t + \mathrm{i}kx), \tag{A1}$$

and for the flow field

$$u(x,y,t) = \hat{u}(y)\exp(\sigma t + \mathrm{i}kx), \tag{A2}$$
$$v(x,y,t) = \hat{v}(y)\exp(\sigma t + \mathrm{i}kx), \tag{A3}$$
$$p(x,y,t) = \hat{p}(y)\exp(\sigma t + \mathrm{i}kx), \tag{A4}$$

where the actual interface position and pressure fields are given by the real part of (A1)–(A4).

Substitution of the normal mode expressions (A2)–(A4) into the linearized governing equations (14)–(15) gives rise to the following differential equations for the amplitude of the vertical component of the perturbed

velocity for each fluid,

$$\left[1-\frac{\nu_1}{(\sigma+\mathrm{i}kU_1)}\left(\frac{d^2}{dy^2}-k^2\right)\right]\left(\frac{d^2}{dy^2}-k^2\right)\hat{v}_1=0, \tag{A5}$$

for fluid 1 and,

$$\left(\frac{d^2}{dy^2}-k^2\right)\hat{v}_2=0, \tag{A6}$$

for fluid 2. Here, $\nu_1=\mu_1/\rho_1$ denotes the kinematic viscosity. Solutions of (A5) and (A6) that vanish far from the interface can be written as

$$\begin{aligned}\hat{v}_1&=c_{11}\exp(ky)+c_{13}\exp(q_1y),\\ \hat{v}_2&=c_{22}\exp(-ky),\end{aligned} \tag{A7}$$

where,

$$q_1=\sqrt{k^2+\frac{\sigma+\mathrm{i}kU_1}{\nu_1}}, \tag{A8}$$

for wavenumber k real and positive and only admitting solutions for which the real part of q_1 is positive.

Writing the boundary conditions in terms of $\hat{v}_1$ and $\hat{v}_2$, the balance of normal stresses (16) at $y=0$ leads to

$$\frac{\mu_1}{k^2}\frac{d^3\hat{v}_1}{dy^3}-\left[3\mu_1+\frac{\rho_1(\sigma+\mathrm{i}kU_1)}{k^2}\right]\frac{d\hat{v}_1}{dy}+\frac{\rho_2}{k^2}(\sigma+\mathrm{i}kU_2)\frac{d\hat{v}_2}{dy}$$
$$+\left[-\gamma k^2-(\rho_1-\rho_2)g\right]\frac{\hat{v}_2}{(\sigma+\mathrm{i}kU_2)}=0. \tag{A9}$$

The zero-tangential stress condition (17) yields

$$\frac{d^2\hat{v}_1}{dy^2}+k^2\hat{v}_1=0, \tag{A10}$$

and the kinematic condition (18) results in

$$\frac{\hat{v}_1}{(\sigma+\mathrm{i}kU_1)}=\frac{\hat{v}_2}{(\sigma+\mathrm{i}kU_2)}. \tag{A11}$$

Substitution of (A7) into (A9)–(A11) leads to a linear homogeneous system of equations for the unknowns c_{11}, c_{13}, c_{22}. For a nontrivial solution, the dispersion relation (19) must be satisfied.

Appendix B: Dimensionless form of the dispersion relations

The dimensionless form of the dispersion relations given above from the various methods of analysis are written here in dimensionless form ignoring surface tension and gravity. In those equations, the velocity of fluid 1 is set equal to U and that of fluid 2 to $-U$. This represents no loss of generality as discussed in the "Results and discussion" section.

The dispersion relation for **IPF** can be obtained from (35) by simply setting the viscosities of both fluids to zero. This yields

$$\rho_1\left(\sigma+\mathrm{i}kU\right)^2+\rho_2\left(\sigma-\mathrm{i}kU\right)^2=0. \tag{B1}$$

With the dimensionless complex growth rate given by

$$\hat{\sigma}=\frac{\sigma}{kU}, \tag{B2}$$

expression (B4) can be written in dimensionless form as

$$\left(\hat{\sigma}+\mathrm{i}\right)^2+r\left(\hat{\sigma}-\mathrm{i}\right)^2=0, \tag{B3}$$

so that the dimensionless growth rate and wavespeed are, respectively,

$$\hat{\sigma}_r=2\frac{\sqrt{r}}{1+r}, \tag{B4a}$$

$$\hat{c}=-\frac{1-r}{1+r}, \tag{B4b}$$

where the density ratio $r=\rho_2/\rho_1=\alpha_2/\alpha_1$ is the only parameter.

For **VPF**, the dimensionless form of (35) is

$$\left(\hat{\sigma}+\mathrm{i}\right)^2+r\left(\hat{\sigma}-\mathrm{i}\right)^2+2\hat{k}\left(\hat{\sigma}+\mathrm{i}\right)+2rm\hat{k}\left(\hat{\sigma}-\mathrm{i}\right)=0, \tag{B5}$$

where the dimensionless wavenumber is

$$\hat{k}=\frac{\nu_1 k}{U}, \tag{B6}$$

and $m=\nu_2/\nu_1$. In this case, the dimensionless growth rate and wavespeed depend on $\hat{k}$, r and m.

For **DM**, relation (34) becomes

$$\left(\hat{\sigma}+\mathrm{i}\right)^2+r\left(\hat{\sigma}-\mathrm{i}\right)^2+4\hat{k}\left(\hat{\sigma}+\mathrm{i}\right)=0. \tag{B7}$$

Here, $\hat{\sigma}$ is determined by $\hat{k}$ and r.

For **ES**, the dispersion relation is (19). For this, we may write

$$Y=\sqrt{1+\frac{\hat{\sigma}+\mathrm{i}}{\hat{k}}}, \tag{B8}$$

and the coefficients

$$\begin{aligned}a_0&=1+4\mathrm{i}\frac{\alpha_2}{\hat{k}}-4\frac{\alpha_2}{\hat{k}^2},\\ a_1&=-2-2\left(\alpha_1-\alpha_2\right),\\ a_2&=2(\alpha_1-\alpha_2)-4\mathrm{i}\frac{\alpha_2}{\hat{k}},\end{aligned}$$

where $\alpha_1=1/(1+r)$ and $\alpha_2=r/(1+r)$. Also in this case $\hat{\sigma}$ depends upon $\hat{k}$ and r.

Finally, for **HM**, relation (22) holds with

$$a_0 = 1 + 4\mathrm{i}\frac{\alpha_2}{\hat{k}} - 4\frac{\alpha_2}{\hat{k}^2} - 4m\alpha_2 - 8\mathrm{i}m\frac{\alpha_2}{\hat{k}},$$
$$a_1 = -1 - 2(\alpha_1 - \alpha_2) + 4\mathrm{i}\frac{\alpha_2}{\hat{k}} - 4\frac{\alpha_2}{\hat{k}^2},$$
$$a_2 = -2 - 4\mathrm{i}\frac{\alpha_2}{\hat{k}} + 4m\alpha_2,$$
$$a_3 = 2(\alpha_1 - \alpha_2) - 4\mathrm{i}\frac{\alpha_2}{\hat{k}}.$$

Therefore, the dimensionless growth rate and wavespeed are determined by $\hat{k}$, r and m in this case.

To compare the results from IPF with those from the theories that consider viscous effects in the graphs of $\hat{k}\hat{\sigma}_r$ versus $\hat{k}$, both sides of expression (B4a) are multiplied by $\hat{k}$. With $\sigma = \hat{\sigma}kU$, the theory for inviscid fluids predicts that the Kelvin-Helmholtz instability is of the Hadamard type, as discussed above.

1. Dimensionless growth rate and wavespeed for long waves

For long waves, i.e. $\hat{k} \to 0$, the leading order terms for the dimensionless growth rate and wavespeed from the various viscous theories match the inviscid limit, given in (B4).

2. Dimensionless growth rate and wavespeed for short waves

For short waves, i.e. $\hat{k} \to \infty$, the dimensionless growth rate and wavespeed tend to the following values.

For **IPF**, the growth rate and wave frequency are given in (B4) for all wavenumbers.

For **VPF**:

$$\hat{\sigma}_r \approx \frac{2r}{\hat{k}}\frac{(1+rm^2)}{(1+rm)^3}, \tag{B9a}$$

$$\hat{c} \approx -\frac{1-rm}{1+rm}. \tag{B9b}$$

For **DM**:

$$\hat{\sigma}_r \approx \frac{r}{\hat{k}}, \tag{B10a}$$

$$\hat{c} \approx -1. \tag{B10b}$$

For **ES**:

$$\hat{\sigma}_r \approx \frac{2r}{\hat{k}}, \tag{B11a}$$

$$\hat{c} \approx -1. \tag{B11b}$$

For **HM**:

$$\hat{\sigma}_r \approx \frac{2r}{\hat{k}}\frac{(1+2rm^2)}{(1+rm)^3}, \tag{B12a}$$

$$\hat{c} \approx -\frac{1-rm}{1+rm}. \tag{B12b}$$

[1] G. G. Stokes, Trans. Cambridge Philos. Soc., **IX**, 8 (1851), (Math. Phys. Papers, 3, pp. 1-141)

[2] D. D. Joseph, T. Funada, and J. Wang, *Potential flows of viscous and viscoelastic fluids* (Cambridge University Press, 2007)

[3] T. Funada, J. Wang, and D. D. Joseph, Atomization and Sprays, **16**, 763 (2006)

[4] J. C. Padrino, D. D. Joseph, T. Funada, J. Wang, and W. A. Sirignano, J. Fluid Mech., **578**, 381 (2007)

[5] S. Dabiri, W. A. Sirignano, and D. D. Joseph, J. Fluid Mech., **605**, 1 (2009)

[6] T. Funada and D. D. Joseph, Int. J. Multiphase Flow, **28**, 1459 (2005)

[7] J. Wang, D. D. Joseph, and T. Funada, J. Fluid Mech., **522**, 383 (2005)

[8] J. Wang, D. D. Joseph, and T. Funada, Phys. Fluids, **17**, 052105 (2005)

[9] D. D. Joseph, J. Belanger, and G. S. Beavers, Int. J. Multiphase Flow, **25**, 1263 (1999)

[10] T. Funada and D. D. Joseph, J. Fluid Mech., **445**, 263 (2001)

[11] R. Asthana and G. S. Agrawal, Phys. A: Stat. Mech. Appl., **382**, 389 (2007)

[12] H. J. Kim, S. J. Kwon, J. C. Padrino, and T. Funada, J. Phys. A: Math. Theor., **41**, 335205 (2008)

[13] J. C. Padrino and D. D. Joseph, Phys. Fluids, **19**, 082105 (2007)

[14] J. C. Padrino, T. Funada, and D. D. Joseph, Int. J. Multiphase Flow, **34**, 61 (2008)

[15] A. Ardekani and D. D. Joseph, Proc. of Nat. Acad. Sci., **106**, 4992 (2009)

[16] H. Kim, T. Funada, D. D. Joseph, and G. M. Homsy, Phys. Fluids, **21**, 074106 (2009)

[17] D. D. Joseph, J. Fluid Mech., **488**, 213 (2003)

[18] T. Funada, D. D. Joseph, T. Maehara, and T. Yamashita, Int. J. Multiphase Flow, **31**, 473 (2004)

[19] H. Lamb, *Hydrodynamics* (Cambridge University Press, 1932)

[20] D. W. Moore, J. Fluid Mech., **6**, 113 (1959)
[21] V. G. Levich, Zh. Eksp. Teor. Fiz., **19**, 18 (1949)
[22] D. W. Moore, J. Fluid Mech., **16**, 161 (1963)
[23] C. Mata, E. Pereyra, J. L. Trallero, and D. D. Joseph, Int. J. Multiphase Flow, **28**, 1249 (2002)
[24] L. D. L. and E. M. Lifshitz, *Fluid Mechanics*, 2nd ed., Course of Theoretical Physics, Vol. 6 (Pergamon Press, Oxford, UK, 1987) (Reprinted in 1989)
[25] X. G. Li and R. S. Tankin, J. Fluid Mech., **226**, 425 (1991)
[26] K. Adham-Khodaparast, M. Kawaji, and B. N. Antar, Phys. Fluids, **7**, 359 (1995)
[27] This method was suggested to us by Prof. W. A. Sirignano.
[28] S. Chandrasekhar, *Hydrodynamic and hydromagnetic stability* (Oxford University Press, Oxford, UK, 1961) (Reprinted by Dover in 1981)
[29] L. E. Johns and R. Narayanan, *Interfacial instability* (Springer-Verlag, New York, 2002)
[30] P. G. Drazin and W. H. Reid, *Hydrodynamics Stability* (Cambridge University Press, Cambridge, UK, 1981)